Uncovering Early Galaxy Evolution in the ALMA and JWST Era
Proceedings IAU Symposium No. 352, 2019
E. da Cunha, J. Hodge, J. Afonso, L. Pentericci & D. Sobral, eds.

doi:10.1017/S1743921319009256

Star-formation efficiency at 600Myr of cosmic time

Mauro Stefanon[1], Ivo Labbé[2], Rychard Bouwens[1] and Pascal Oesch[3]

[1]Leiden Observatory, University of Leiden, Niels Bohrweg, 2 - 2333CA Leiden - The Netherlands
email: stefanon@strw.leidenuniv.nl

[2]Centre for Astrophysics and SuperComputing, Swinburne, University of Technology, Hawthorn, Victoria, 3122, Australia

[3]Observatoire de Genève, 51 Ch. des Maillettes, 1290 Versoix, Switzerland

Abstract. Current observations suggest an accelerated evolution of the cosmic star formation rate density for $8 < z < 10$, indicating that galaxy assembly experienced an extremely intense phase during the first ~ 600 Myr years of cosmic time. We performed a systematic search of ultrabright star-forming galaxies at $z \sim 8$ over the COSMOS/UltraVISTA survey, identifying 16 candidate Lyman-break galaxies. The still large uncertainties on the associated volume density do not yet allow us to ascertain whether a different star-formation efficiency (SFE) existed at early cosmic epochs. Leveraging the deepest Spitzer/IRAC data available from the GREATS program over the CANDELS/GOODS fields, we also constructed stacked SEDs of sub-L^* LBGs at $z \sim 8$. We find extreme nebular line emission (EW$_0$(Hα) ~ 1000 Å), high specific star-formation rates (~ 10/Gyr) and indication of an inverse Balmer break. These results point toward very young ages (< 100 Myr), and, combined with measurements at lower redshifts, that the SFE evolved only marginally during the first ~ 1.5 Gyr of cosmic history.

1. Introduction

In the last decade, the synergy between the major Observatories combined with efficient photometric selection techniques have allowed us to probe galaxy formation as far as the early re-ionization epoch, identifying $\sim$10k galaxies at $z > 4$, with $\gtrsim 500$ candidates at $8 \lesssim z \lesssim 11$ (Ellis *et al.* 2013; Oesch *et al.* 2013, 2014, 2018; Schenker *et al.* 2013; Schmidt *et al.* 2014; Bouwens *et al.* 2015, 2016; Finkelstein *et al.* 2015b; McLeod *et al.* 2016; Ishigaki *et al.* 2018). These remarkable observational efforts have allowed us to gain insights on the evolution of the star-formation rate density (SFRD), stellar mass density and specific star-formation rate (sSFR) up to $z \sim 8-10$ (Labbé *et al.* 2013; Stark *et al.* 2013; González *et al.* 2014; Smit *et al.* 2014; Salmon *et al.* 2015; Faisst *et al.* 2016; Duncan *et al.* 2014,; Song *et al.* 2016; Davidzon *et al.* 2018).

The redshift range $z \sim 8-11$ is of particular interest. Controversial results on whether the efficiency of star formation evolved or not at early cosmic epochs still exist both among observations (e.g., Behroozi *et al.*, 2013; Finkelstein *et al.* 2015a; Harikane *et al.* 2016, 2018; Stefanon *et al.* 2017a) and among models (Behroozi *et al.* 2018; Tacchella *et al.* 2018). Further constraints to the star-formation efficiency come from the study of the bright end of the UV luminosity function (e.g., Finlator *et al.* 2011; Mason *et al.* 2015; Mashian *et al.* 2016). Indeed, the recent spectroscopic confirmation of one ultra-bright $M_{\rm UV} = -22.1$ mag galaxy at $z = 11.1$ (GN-z11 - Oesch *et al.* 2016) suggests that galaxy assembly could have been well under way at just ~ 400 Myr of cosmic time, challenging current models of galaxy evolution (e.g., Mutch *et al.*, 2016).

To further our understanding of galaxy assembly at early cosmic epochs, we need to successfully overcome challenges at different luminosity regimes. For $L \lesssim L^*$, one factor that is currently limiting the estimates of the physical parameters of $z \gtrsim 8$ galaxies is the lack of deep observations at rest-frame optical wavelengths, currently only probed by Spitzer/IRAC. Observational progress at the very bright end, instead, has been relatively slow due to the combined effects of the small field of view of the HST/WFC3 camera and of the low surface densities of bright galaxies at $z \gtrsim 8$, with remarkable exceptions from the BoRG/HIPPIES programs (Trenti *et al.* 2011; Yan *et al.* 2011) and from the Hubble Frontier Fields, CLASH and RELICS initiatives.

2. Bright galaxies at $z \sim 8$

An alternative approach in the search for bright LBGs at $z \gtrsim 8$ consists in analyzing the ground-based wide-field surveys such as COSMOS/UltraVISTA and UKIDSS/UDS, with deep (~ 26 mag) broad wavelength coverage ($0.3 - 5\mu$m - e.g., Bowler *et al.* 2012, 2014, 2015, 2017; Stefanon *et al.* 2017b).

Our group has performed a systematic search for the brightest, most luminous, star-forming galaxies at $z \sim 8$ over the ~ 0.7 square degrees of COSMOS/UltraVISTA field, selecting them as Y-dropouts. Our search identified 16 bona-fide galaxies with redshifts in the range $7.4 \lesssim z \lesssim 8.7$ and $-22.5 \lesssim M_{\rm UV} \lesssim -21.4$ mag. These luminosities make them among the most luminous galaxies identified at these redshifts, the brightest identifications based on such a significant range of multi-wavelength observations. Our SED analysis shows that 10 of these galaxies have a confidence of $> 95\%$ of being robust $z \sim 8$ star-forming galaxies. One of the currently open questions is whether the bright end of the UV LF follows a Schechter or a double power-law form. A double power-law form would imply a more efficient star-formation compared to the faster decline of the Schechter exponential form. However, our analysis combining our results with the volume densities of Bouwens *et al.* (2015) does not yet allow us to distinguish between these two forms (Stefanon *et al.*, 2019a, in press).

3. Probing the specific star-formation rate at $z \sim 8$

The recently completed GOODS Re-ionization Era wide-Area Treasury from Spitzer (GREATS) program (PI: Labbé - Stefanon *et al.* 2019b, in preparation) provides full-depth coverage in the 3.6μm and 4.5μm bands with depth of ~ 150 hours over ~ 150arcmin^2, corresponding to nominal ultradeep limits of ~ 27.0 and 26.7 mag (AB, 5σ), enabling simultaneous detection in the 3.6μm and 4.5μm bands for more than half of the $z \sim 8$ LBGs identified in the GOODS fields. Using these data we built stacked SEDs from 119 robust LBG candidates at $z \sim 8$ segregated into four different luminosity bins to study their main physical parameters (SFR, age and stellar mass). The stacked SEDs are characterized by two main features:

Red $[3.6] - [4.5]$ *color.* The first notable feature is a red $[3.6] - [4.5] > 0$ mag color. Previous works have interpreted a red color at similar redshifts as the effect of nebular Hβ+[O III] emission entering the 4.5μm band at $z \sim 7.3$ (e.g., Schaerer & de Barros 2009; Labbé *et al.* 2013). Under this hypothesis, we estimate extreme rest-frame equivalent width EW(Hβ+[OIII]) ~ 1000Å (assuming the line ratios of Anders & Fritze-v. Alvensleben 2003 for sub-solar metallicity ($Z = 0.2 Z_\odot$), and assuming a flat f_ν continuum), consistent with other estimates at similar redshifts (Labbé *et al.* 2013; Smit *et al.* 2014, 2015), and suggesting either young ages, low metallicities high rates of star formation or a combination thereof.

https://doi.org/10.1017/S1743921319009256 Published online by Cambridge University Press

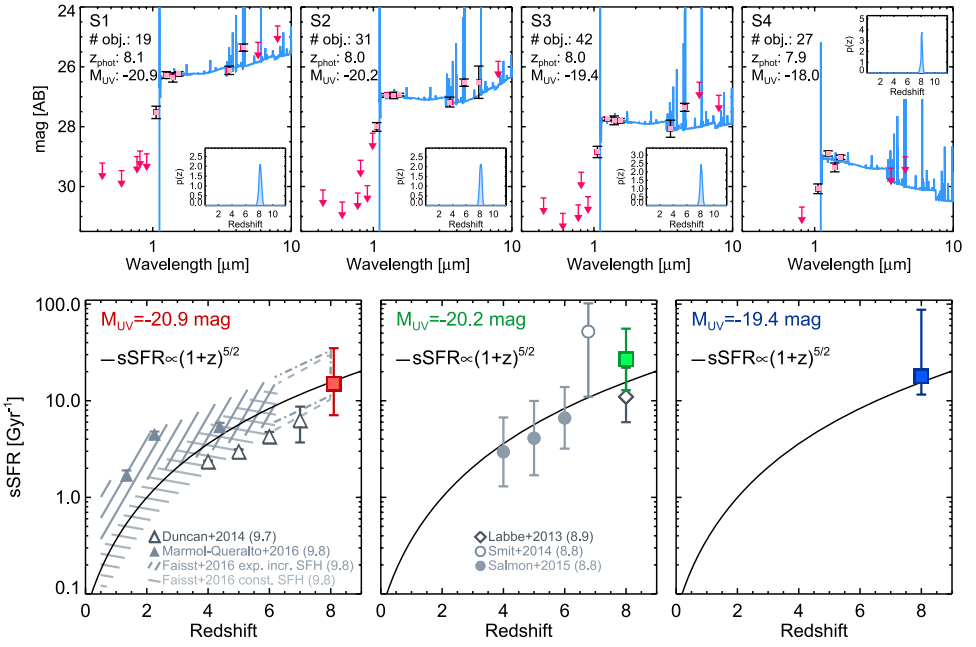

Figure 1. Top row: Stacked SEDs resulting from our analysis of $L < L^*$ LBGs at $z \sim 8$. Each panel refers to a stack at a different luminosity, as indicated by the label at the top-left corner of each panel. In each panel, the filled red squares with errorbars mark the stacked photometry, while the red arrows represent 2σ upperlimits. All SEDs present red $[3.6] - [4.5] > 0$ mag colors; the SEDs of the three less luminous stacks present blue $H_{160} - [3.6] < 0$ mag color, suggesting young stellar populations. **Bottom row:** Evolution of the sSFR with redshift. The measurements from the stacking analysis are presented in the panels according to their $M_{\rm UV}$, indicated at the top. In each panel we also plot recent estimates of the sSFR at high redshifts from the literature, as indicated by the legends at the bottom, segregated according to their stellar mass, quoted in parenthesis in log scale. The black curve corresponds to the evolution of the sSFR from the toy model of Dekel *et al.* (2013), of the form sSFR $\propto (1+z)^{5/2}$, as expected from cold gas inflow that follows the hierarchical merging of the dark matter halos. The overall good match of the curve to the observations suggests a scenario where the star-formation efficiency did not strongly evolve with cosmic time.

Blue $H - [3.6]$ color. Perhaps, the most intriguing feature of the stacked SEDs is the blue $H_{160} - [3.6] < 0$ color. At redshifts $z \sim 8$ the 3.6μm band covers the rest-frame wavelengths around the Balmer/4000Å break; the measured blue color suggests very young ages of the stellar populations. More accurate estimates of the stellar continuum red-wards of the Balmer Break would benefit from 8.0μm-band measurements, poorly constrained in our sample.

An SED analysis assuming a constant SFH results in ages of < 100 Myr and correspond to sSFR of $10 - 35\,{\rm Gyr}^{-1}$, consistent with those observed at $z \sim 7 - 8$ LBGs from broad band photometry (Labbé *et al.* 2013; Smit *et al.* 2014; Castellano *et al.* 2017). When considered together with estimates at lower redshifts, our new measurements indicate an increasing sSFR with redshift out to $z \sim 8$. Remarkably, the similarity between the evolution of the sSFR and that of the specific accretion rate of the dark matter halos at $3 < z < 8$, that we show in Figure 1, suggests that at high redshifts galaxy formation might be dominated by the assembly of cold gas, driven by the hierarchical formation of the dark matter halos and therefore that the evolution with redshift of the $M_\star/M_{\rm halo}$ ratio should be marginal.

https://doi.org/10.1017/S1743921319009256 Published online by Cambridge University Press

Acknowledgements

We are delighted to acknowledge the contributions of our collaborators Ivo Labbé, Rychard Bouwens, Pascal Oesch, Garth Illingworth and the UltraVISTA team.

References

Anders, P. & Fritze-v. Alvensleben, U. 2003, *A&A*, 401, 1063
Behroozi, P. & Silk, J. 2018, *MNRAS*, 477, 5382
Bernard, S. R., Carrasco, D., Trenti, M., *et al.* 2016, *ApJ*, 827, 76
Bouwens, R. J., Illingworth, G. D., Oesch, P. A., *et al.* 2015, *ApJ*, 803, 34
Bouwens, R. J., Oesch, P. A., Labbé, I., *et al.* 2016, *ApJ*, 830, 67
Bowler, R. A. A., Dunlop, J. S., McLure, R. J., & McLeod, D. J. 2017, *MNRAS*, 466, 3612
Bowler, R. A. A., Dunlop, J. S., McLure, R. J., *et al.* 2012, *MNRAS*, 426, 2772
—. 2014, *MNRAS*, 440, 2810
—. 2015, *MNRAS*, 452, 1817
Calvi, V., Trenti, M., Stiavelli, M., *et al.* 2016, *ApJ*, 817, 120
Castellano, M., Pentericci, L., Fontana, A., *et al.* 2017, *ApJ*, 839, 73
Davidzon, I., Ilbert, O., Faisst, A. L., *et al.* 2018, *ApJ*, 852, 107
de Barros, S., Oesch, P. A., Labbé, I., *et al.* 2018 - submitted, *ApJ*
Dekel, A., Zolotov, A., Tweed, D., *et al.* 2013, *MNRAS*, 435, 999
Duncan, K., Conselice, C. J., Mortlock, A., *et al.* 2014, *MNRAS*, 444, 2960
Ellis, R. S., McLure, R. J., Dunlop, J. S., *et al.* 2013, *ApJL*, 763, L7
Faisst, A. L., Capak, P., Hsieh, B. C., *et al.* 2016, *ApJ*, 821, 122
Finkelstein, S. L., Ryan, R. E., Papovich, C., *et al.* 2015a, *ApJ*, 810, 71
Finkelstein, S. L., Song, M., Behroozi, P., *et al.* 2015b, *ApJ*, 814, 95
Finlator, K., Oppenheimer, B. D., & Davé, R. 2011, *MNRAS*, 410, 1703
González, V., Bouwens, R., Illingworth, G., *et al.* 2014, *ApJ*, 781, 34
Harikane, Y., Ouchi, M., Ono, Y., *et al.* 2016, *ApJ*, 821, 123
Harikane, Y., Ouchi, M., Ono, Y., *et al.* 2018, *PASJ*, 70, S11
Ishigaki, M., Kawamata, R., Ouchi, M., *et al.* 2018, *ApJ*, 854, 73
Labbé, I., Oesch, P. A., Bouwens, R. J., *et al.* 2013, *ApJL*, 777, L19
Livermore, R. C., Trenti, M., Bradley, L. D., *et al.* 2018, *ApJL*, 861, L17
Lotz, J. M., Koekemoer, A., Coe, D., *et al.* 2017, *ApJ*, 837, 97
Mashian, N., Oesch, P. A., & Loeb, A. 2016, *MNRAS*, 455, 2101
Mason, C. A., Trenti, M., & Treu, T. 2015, *ApJ*, 813, 21
McLeod, D. J., McLure, R. J., & Dunlop, J. S. 2016, *MNRAS*, 459, 3812
McLeod, D. J., McLure, R. J., Dunlop, J. S., *et al.* 2015, *MNRAS*, 450, 3032
Morishita, T., Trenti, M., Stiavelli, M., *et al.* 2018, *ApJ*, 867, 150
Oesch, P. A., Labbé, I., Bouwens, R. J., *et al.* 2013, *ApJ*, 772, 136
Oesch, P. A., Bouwens, R. J., Illingworth, G. D., *et al.* 2014, *ApJ*, 786, 108
Oesch, P. A., Brammer, G., van Dokkum, P. G., *et al.* 2016, *ApJ*, 819, 129
Oesch, P. A., Bouwens, R. J., Illingworth, G. D., *et al.* 2018, *ApJ*, 855, 105
Salmon, B., Papovich, C., Finkelstein, S. L., *et al.* 2015, *ApJ*, 799, 183
Schenker, M. A., Robertson, B. E., Ellis, R. S., *et al.* 2013, *ApJ*, 768, 196
Schmidt, K. B., Treu, T., Trenti, M., *et al.* 2014, *ApJ*, 786, 57
Smit, R., Bouwens, R. J., Labbé, I., *et al.* 2014, *ApJ*, 784, 58
Song, M., Finkelstein, S. L., Ashby, M. L. N., *et al.* 2016, *ApJ*, 825, 5
Stark, D. P., Schenker, M. A., Ellis, R., *et al.* 2013, *ApJ*, 763, 129
Stefanon, M., Labbé, I., Bouwens, R. J., *et al.* 2017b, *ApJ*, 851, 43
Stefanon, M., Labbé, I., Bouwens, R. J., *et al.* 2019a, arXiv e-prints, arXiv:1902.10713
Stefanon, M. *et al.* 2019b - in prep., *ApJ*
Tacchella, S., Bose, S., Conroy, C., *et al.* 2018, *ApJ*, 868, 92
Trenti, M., Bradley, L. D., Stiavelli, M., *et al.* 2011, *ApJL*, 727, L39
Waters, D., Wilkins, S. M., Di Matteo, T., *et al.* 2016, *MNRAS*, 461, L51
Yan, H., Yan, L., Zamojski, M. A., *et al.* 2011, *ApJL*, 728, L22